J Ther Eng, Vol. 11, No. 5, pp. 1−15, September, 2025

Journal of Thermal Engineering
Web page info: https://jten.yildiz.edu.tr
DOI: 10.14744/thermal.0000000

Research Article

Highly viable nanoparticle based Thermal Interface Materials (TIM) for electronics device cooling applications

S Uma MAHESHWARI[1,*], A. Brusly SOLOMON[2], G. THILAGAVATHI[3], Madhukar HEMAMALINI[4], D. ILLAKKIAM[5]

[1]Department of Physics, Mother Teresa Women's University, Kodaikanal, 624101, India
[2]Micro and Nano Heat Transfer Lab, Centre for research in material science and thermal management, Division of Mechanical Engineering, Karunya Institute of Technology and Sciences, Karunya Nagar, Coimbatore, 641001, India
[3]Dr. M.G.R Govt. Arts and Science College for Women, Villupuram,605401, India
[4]Department of Chemistry, Mother Teresa Women's University, Kodaikanal, 624101, Indıa
[5]Department of Biotechnology, Mother Teresa Women's University, Kodaikanal, 624101, India

ARTICLE INFO

Article history
Received: 10 August 2024
Accepted: 13 September 2024

Keywords:
Bond Line Thickness; Effective Thermal Contact Resistance; Heat Transfer Applications; Nanoparticles; Thermal Interface Material

ABSTRACT

High performance interface materials (TIMs) were developed using various nanoparticles and paraffin wax. An indigenous test set up was fabricated using aluminium heat sink and copper plates as heating plate for measuring effective thermal contact resistance ($R_{th,\,eff}$) of prepared TIMs to evaluate their thermal performance. Chrome-Alumel thermocouples were used for measuring the temperature. Furthermore a relative study of effective thermal contact resistance of prepared (TIMs) was carried out to evaluate their performance. The nanoparticle chosen for present distinctive study were SiO_2, Al_2O_3, CuO, GO, rGO. The TIM samples were synthesized by blending 6 wt% of assorted nanoparticles in 5 ml base fluid of paraffin wax. They were uniformly mixed using ultra sonicator to create a smooth and fine paste based TIM. The resulting paste (TIMs) was applied as an ultra-thin layer between the copper heater and aluminium sink of the indigenously designed and fabricated test rig. Power inputs for experiments were 25, 50 and 75W. Experimental studies were done at reduced pressure (RP) and full pressure (FP) applied by completely loosening and tightening the screws of the aluminium heat sink. . Addition of (SiO_2, Al_2O_3, CuO, GO and rGO) nanoparticles to the base fluid paraffin wax significantly decreases the effctive thermal resistance to a large extent as the added nano parcticles helps in better heat conduction due to their enhanced total surface area leading to more effcetive heat evacuation. Enhanced results are observed at full pressure, at reduced pressure drastic increment in ($R_{th,\,eff}$) occurs due to improper gap filling. These results significantly depicts the importance of bondline thickness in performance of TIM. Interestingly siliica based TIM gives the best performance of heat transference to ambience at 50 W power input ($R_{th,\,eff}$ = 0.46^{0}C/W) and slightly becomes inferior to GO at higher power input. GO based TIM shows the best results at higher power of 75 W, its $R_{th,\,eff}$ being 0.51^{0}C/W.

Cite this article as: Maheshwari SU, Solomon AB, Thilagavathi G, Hemamalini M, Illakkiam D. Highly viable nanoparticle based Thermal Interface Materials (TIM) for electronics device cooling applications. J Ther Eng 2025;11(5):1−15.

***Corresponding author.**
*E-mail address: phduma13@gmail.com

This paper was recommended for publication in revised form by Editor-in-Chief Ahmet Selim Dalkılıç

INTRODUCTION

With the advent of low dimensional physics, new generation of electronic products are in nano dimensions packed with more power and enhanced performance in lesser packaged space, hence the greater necessity of thermal management within the overall products design becomes important. It is already known that when two rough surfaces meet, uneven interfaces are formed. These uneven surfaces are not suave and flat which causes diminished contact area. Now the actual interface only has distorted micro-contacts. The size of the impact region depends on different factors, including the roughness of the structures, the internal properties and the impact pressure. Therefore, elastic, flatness of solids and plastic properties and physical strain regulate the distribution of impact spots. As result of this micro and macro gaps and voids that are sealed up by the materials, such as air, are created. Technically the conventional heat transfer methods like conduction, convection, radiation happening through a solid-solid interface is dependent on interface type [1]. Hence, arises the true need for Thermal Interface materials. The specification of suitable thermal interface material (TIM) for a particular product application is an important part of this thermal engineering work. The emerging survey comprises a wide range of heat transfer technologies which are mechanisms for the conductive cooling which cooling of an electrical system and thermal dissipation material, such as a heat sink or a circuit board. More precisely, the innovation involves a stand-alone, form-stable film that is melted or softens within the temperature range or spectrum of the electronic part in order to properly adhere to thermal interfaces for the improved transfer of heat from the electronic to thermal dissenting components [2]. The Phase Change Materials (PCM) exhibits the good thermal behaviour of grease and possess flexibility of an elastomer pad. PCMs undergo phase change with temperature shifts and convert into liquid state with increasing temperature which is feasible for TIM fabrication. These include paraffin waxes or silicon-based materials. By adding metal nano filler particles, the thermal performance of PCM gets escalated [3, 4].

Scientist reported the higher efficacy of thermal transmission of aluminium coated spherical particles of Al_2O_3 dispersed in paraffin wax as a phase-change thermal interface material [5]. Promising research in the field of elastomers based TIM was carried out by a team of researchers; they synthesized copper nanowire- filled soft elastomer composite as thermal interface materials. [6].Carbon based materials are becoming the choice in myriad of applications due to their novel properties, grapheme being becoming the most researched one. In this league scientists incorporated a thin commercially available paper with water dispersible graphene paste to fabricate a novel TIM. The prepared TIM exhibited good thermal and mechanical properties [7]. Using liquid-phase exfoliation technique eminent researchers prepared graphene-multilayer graphene nanocomposite for thermal efficient TIM applications. The results strongly suggested the exponential increase in thermal conductivity K of the composite [8]. Further to capitalize the maximum benefits of excellent thermal properties of graphene a group of scientist developed few-layer Graphene (FLG) composite, where FLG was prepared by the interlayer catalytic exfoliation (ICE) method. The thermal and mechanical characterization studies demonstrated feasibility of FLG composites as commercially reliable TIMs. The thermal interface resistance between FLG composite TIMs and copper was found to be marginally low in comparison to many commercial TIMs [9]. Researchers fabricated epoxy resin (ER) modified nano-series rGO based TIM and investigated the influence of types of rGO nano-series functional groups on the obtained thermal conductivity of TIM. The thermal conductivity and calculated thermal boundary resistance results proved the greater role of carboxyl groups in enhancing phonon transport at the interface between the graphene base plane and ER.[10]. Scientists designed a simulation method for creating a perfect system design for effective thermal management. An experimental set-up for static measurements is presented that evaluates the thermal conductivity and phase separation resistance of thermal materials (eg, glue, solder, washers or pastes) [11].

Scientist working in the field of thermal science investigated densely stacked vertically multi-walled carbon nanotube arrays as thermal interface materials. The results show that the physically bonded interface via van der wall adhesion had a conductivity of around 105 W / m^2K. It also shows that by bonding the free end CNTs to the target surface with a thin layer of indium weld, the conductivity can be increased to a greater extent [12]. Sreekant narumanchi and group extensively investigated the thermal performance of selected thermoplastics and phase change materials using the ASTM stabilization method and transient laser flash method. The experimental results on thermal resistance were carried out in the context of cooling automotive electronics. The results of the numerical finite element modelling greatly emphasize the importance of the thermal resistance of the TIM layer on the maximum temperature in the IGBT packet [13]. Eminent researchers investigated interfacial thermal resistance (ITR) between the TIM and aluminium surface by using the time domain thermo reflectance method. The ITR dramatically escalated due the depletion of filler layers present adjacent to the aluminium surface. This implies the importance to prevent formation of Filler Depletion Layer in the future thermal management of integrated devices [14]. Electrospun polyamide nanocomposite incorporated with rGO-Ag hetero structured nanoparticles were fabricated. The composites showed excellent thermal conductivity behaviour due the superior thermal conductivity of graphene fillers. All the thermal parameters including thermal conductivity and glass transition temperature of (Ag/rGO)/PI nano composites increased tremendously with increment of loading of Ag/rGO fillers [15]. TIMs are used in melange applications,

including machines, electronic electronics, telephone systems, LED lighting goods, green energy products, vehicles, military and manufacturing equipment and medical instruments. LEDs, thin film photovoltaic, automotive and medical devices, with slower development in mature electronics, military and automobile industries, are anticipated for the fastest rising areas. New innovations like phase change and metallic TIMs are leading in particular for usage at high temperatures, accompanied by adhesives in more conventional forms. The LED framework is expected to dominate the lighting market and over the next 10 years the TIM application is projected to be the fastest increasing and influential project. In recent times elastomeric pads are used anticipated to be the dominant type of TIM [16]. The literature explored above is represented in tabular manner concisely to explore the rationale of carrying out this present study.

Scope of the Present Study

According to the literature reported in our paper, various work involving filler materials like Aluminium, Go, rGO and copper nanowires have been studied for thermal conductivity. The materials have been prepared using mélange of methods including electrospinning and vertical aligned nano arrays. Thermal conductivity studies have been extensively studied. Not much importance was given in the study of effective thermal contact resistance, bond line thickness, PCMs as base fluid and pressure exerted by the TIM to optimize bond line thickness. In this league a deep cut-through study was carried out to highlight the importance of temperature, pressure, the nature of filler particle, and bond line thickness which further affects the effective thermal contact resistance. Table 1 presents the quantitative exploration of literature study.

EXPERIMENTAL METHODS

Preparation of Thermal Interface Material

The silicon dioxide nanoparticle was prepared by chemical sol-gel method. The aluminium dioxide, copper oxide, graphene oxide and Silver- reduced graphene oxide nanoparticles were purchased from Techonano Taiwan to be used as filler particles. The size of all nanoparticles was in the range of 50-100 nm. The paraffin wax was supplied by Loba Chemical, India. Various samples of TIM were prepared by mixing 6 wt% of SiO_2, Al_2O_3, CuO, GO, rGO nanoparticles individually mixed in 5ml of paraffin wax and the samples were magnetically stirred first [17] . Then the mixture was sonicated for 30 minutes using ultra sonicator for uniform dispersion of nanoparticles in liquid Paraffin wax.. The optimal wt% used in the present study is chosen based on our previous experimental results reported in "Development of Low Resistance Thermal Interface Material (TIM) Using Nanomaterials" published in the International Journal of Engineering Science Invention. The formed fine paste was spread as a thin layer over the copper heater and sandwiched between aluminium sink

Table 1. Development of Thermal Interface Materials in Recent Years

S. No	Author	Materials used	Interpretation
1.	Mao D, Xie J, Sheng G, Ye H, Yuen MM, Fu XZ, Sun R and Wong CP [5]	Paraffin wax as base fluid and alumina and Al_2O_3 as filler particle	Alumina as filler particle shows the best thermal conductivity of 1.6743 W/mK compared to only paraffin wax which has thermal conductivity of 0.1504 W/mK
2.	Bhanushali S, Ghosh PC, Simon GP and Cheng W [6]	Flexible elastomer composite embedded copper nanowires.	The matrix showed a thermal conductivity of 3.1 W mK^{-1} which decreased with increasing temperature.
3.	Shahil KMF, Balandin AA [8]	Natural graphite as filler particle and aqueous sodium cholate solution mixed with epoxy as base fluid	The thermal conductivity of the base fluid increased from an initial value of ~5.8 W/mK to K = 14 W/mK at the small loading f = 2%.
4	Park W, Guo Y, Li X, Hu J, Liu L, Ruan X and Chen YP [9]	Graphene as filler particle and epoxy as base material.	The thermal conductivity increases as the filler concentration increased from 0 to 10 %. The highest thermal conductivity is measured to 3.87 ± 0.28 W/mK at 10 vol % at room temperature
5.	Sun Y, He Y, Tang B, Tao C, Ban J and Jiang L [10]	RGO as filler particle and epoxy as base material.	The thermal conductivity of the prepared TIMs was found to be 5.9$Wm^{-1}K^{-1}$.
6.	Tong T, Zhao Y, Delzeit L, Kashani A [12]	Multiwalled CNT arrays grown over Si substrate.	Thermal conductivity was measured around 10^6 W/m^2K
7.	Guo Y, Yang X, Ruan K, Kong J, Dong M, Zhang J, Gu J, and Guo Z [15]	Electrospun Ag/rGO/ Polyimide nanocomposite as TIM	(Ag/rGO)/PI nanocomposite showed a maximum thermal conductivity of 2.12 W/(m K)

of the inbuilt test rig as shown in figure 1. The thickness of TIM spread at complete tightened screws was measured around 30 μm, as measured by a micrometre. At reduced pressure (RP) the thickness was observed to be 42 μm. Experiments were carried out at reduced pressure (RP) and full pressure (FP) which was created by completely loosening and tightening the screws of the aluminium sink. Power inputs were varied as 25, 50 and 75W.the figure 2 represent prepared nanofluids.

To improve the uniform dispersion of the nanoparticles in the base fluid, the mixture was subjected to ultrasonic agitation up to 30 minutes and dispersion was ensured using SEM images of the dried paste at periodic intervals. The stability of nanoparticles was checked using visual observation method. The data in days for which the nanofluids was stable is reported below.

Most of the nanoparticles showed high stability when stored as nanofluids in room temperature before getting precipitated. In our observation aluminium and copper

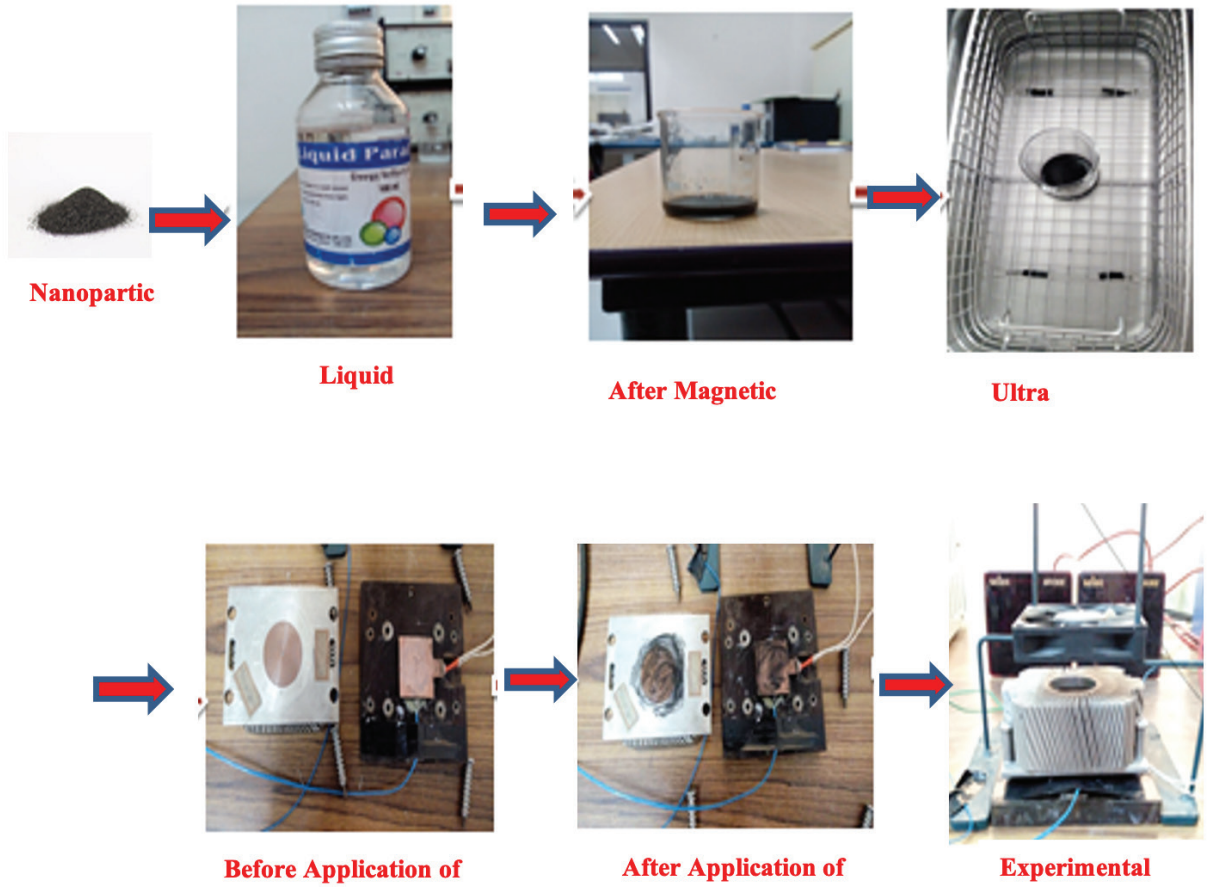

Figure 1. Preparation of TIM and Its Experimental Set Up.

Figure 2. Shows prepared nanofluids of (A) CuO, (B) SiO_2, (C) GO, (D) rGO, (E) Al_2O_3.

Table 2. The Stability of Prepared Nanofluids in Days

S. No	Nanofluid	Stability in Days
1	SiO_2	30
2	Al_2O_3	72
3	CuO	70
4	rGO	55
5	GO	62

oxide nanofluids were the most stable nanoparticles and rGO and GO nanofluids represented similar and high stability. SiO_2 nanofluids showed least stability comparatively. The SEM images taken shows that the nanoparticles are dispersed uniformly even after ten days which can be witnessed in figure 3**.**

Test Set Up

Thermal experiments were carried to determine effective thermal contact resistance (Rth, eff) of various samples. Figure 4 shows schematic of the test rig.

Effective thermal contact resistance ($R_{th,\ eff}$) is calculated for prepared TIM using given equation.

$$R_{th,\ eff} = R_{th} + R_{th0,}\ \text{Cu-TIM} + R_{th0},\ \text{Al-Air}$$

Where,

R_{th} = Thermal resistance of TIM material

R_{th0}, Cu-TIM = Thermal interface resistance between the copper heater block and thermal interface material

R_{th0}, TIM-Al = Thermal interface resistance between the aluminium heat sink and thermal interface material

R_{th0}, Al-Air = Thermal interface resistance between the aluminium heat sink and air

In Figure the details of the experimental set up for measuring $R_{th,\ eff}$ is given.

The above given test rig (Fig. 5) represents the schematic of heat path established between the heater and sink and thermal interface materials bridging the rough surface existing between them. The alternating current (AC) system provides power to the heater cartridge (CH) which in turn raises the temperature of the copper heater

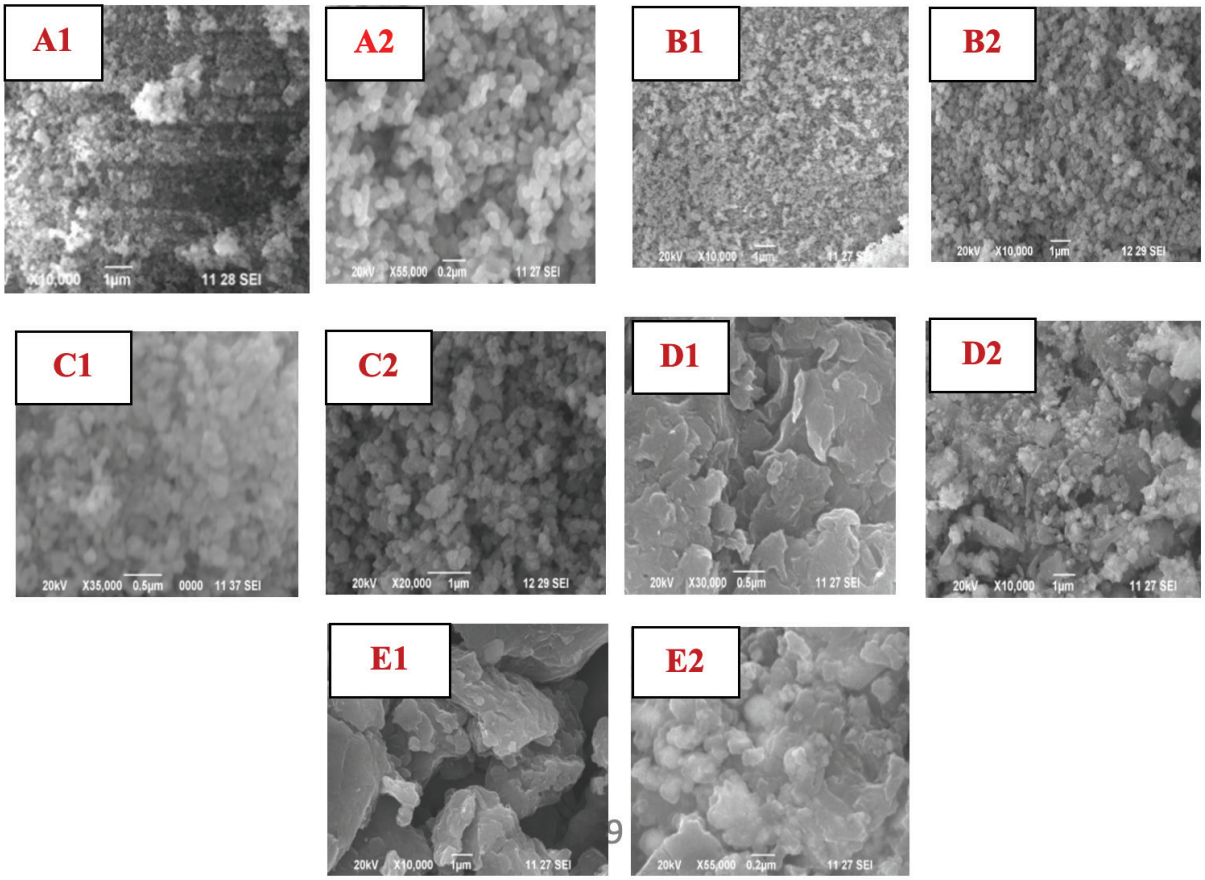

Figure 3. Shows SEM images of dried samples of (A1&A2) SEM images of dried paste of Al_2O_3 after day 1 and day 10 (B1&B2) CuO after day 1 and day 10 (C1&C2) SEM images of dried samples of SiO_2 after day 1 and day 10 (D1&D2) SEM images of dried samples of GO after day 1 and day 10 (E1&E2) SEM images of dried samples of rGO after day 1 and day 10.

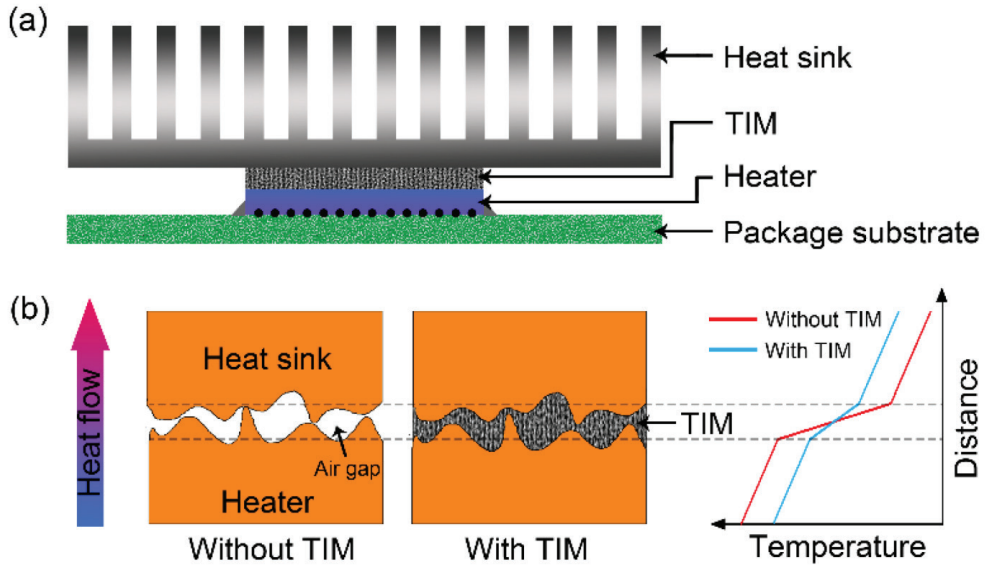

Figure 4. Schematic for Test Set Up.

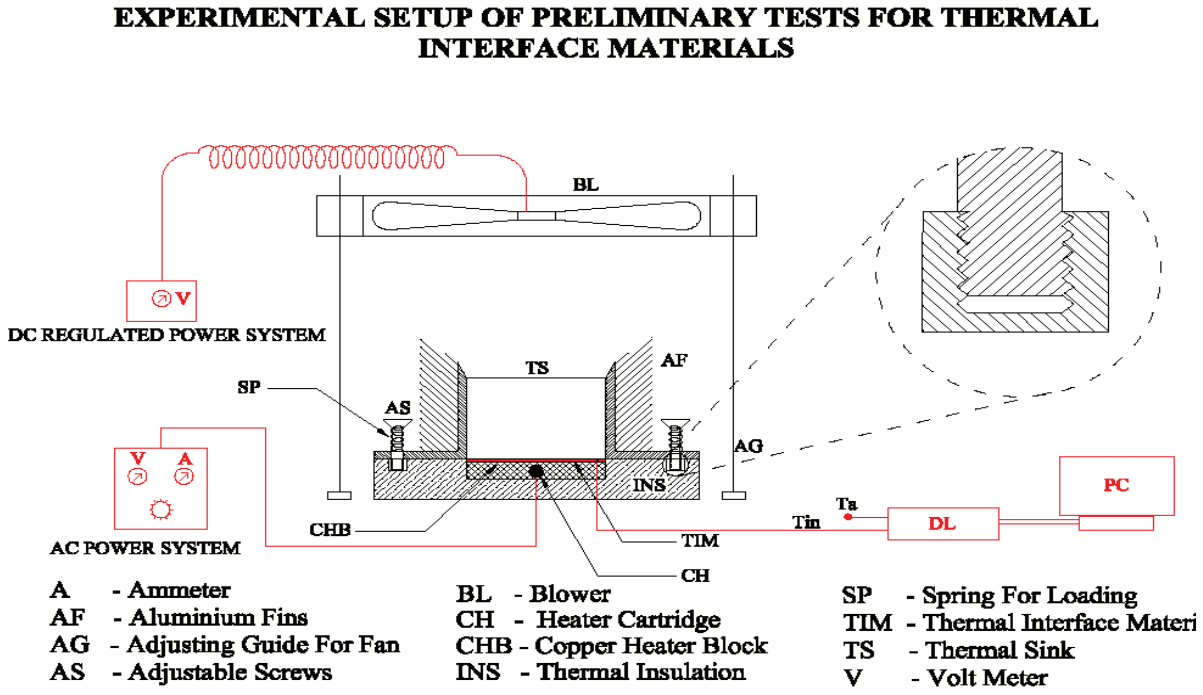

Figure 5. Experimental Setup of Preliminary Tests for Thermal Interface Material.

block (CHB), the elevated temperature being sensed and recorded using the Chrome-Alumel thermocouple system. The uncertainty of the temperature measurement is ± 0.2 Degree Celsius including the uncertainty in the voltmeter ± 0.1 Degree Celsius.

Uncertainty in power and resistance are calculated using following equations and the result is tabulated in table 3

$$\frac{\Delta p}{p} = \sqrt{(\Delta V/V)^2 + (\Delta \mathrm{I}/\mathrm{I})^2}$$

$$\frac{\Delta R}{R} = \sqrt{(\Delta T/T)^2 + (\Delta \mathrm{P}/\mathrm{P})^2}$$

The sensitivity of temperature sensors was measured at ±0.2 °C. A strong aluminium block with multiple close

Table 3. Uncertainty Calculation of Power and Resistance

S. No	Heat Input In Watts	Uncertainty In Power	Uncertainty In Resistance
1	25	2.8%	3.2%
2	50	2.2%	2.6%
3	75	1.6%	1.9%

Table 4. Sensitivity of Devices

S. No	Device	Sensitivity
1.	Temperature sensor	±0.2 °C.
2.	Voltmeter	± 0.1 °C.

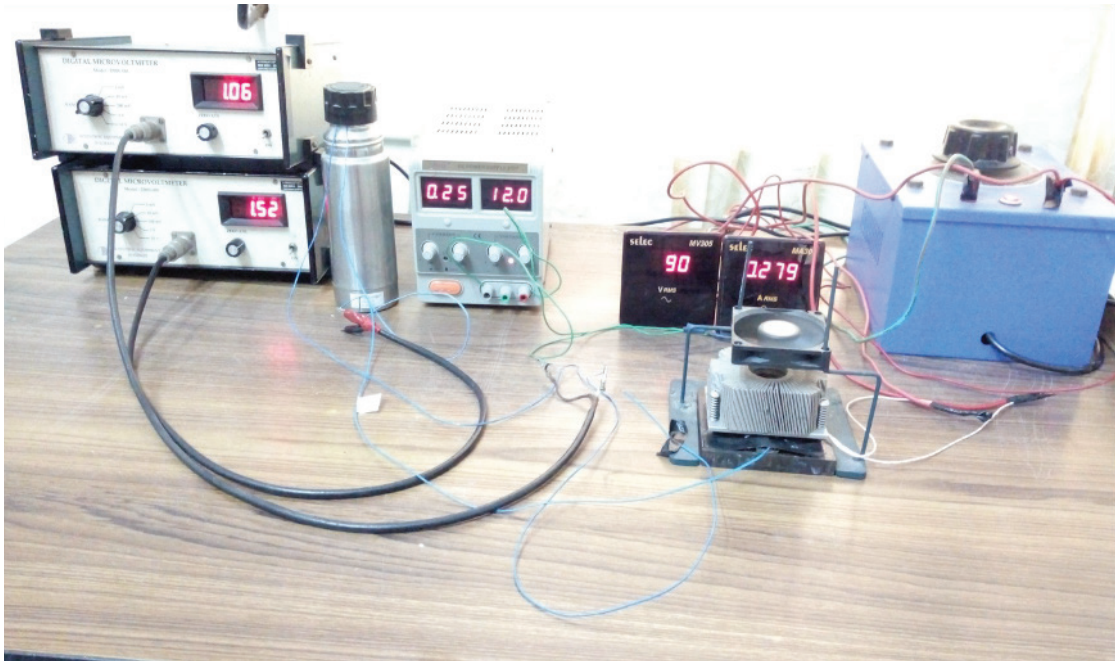

Figure 6. Shows the Instrumentation of Thermal Interface Material Set-up.

stacked fins precisely noted as Aluminium fins (AF) was used as thermal sink (TS). It is fixed to the copper heater block using adjustable screws (AS) and loading spring (SP). TIM is applied over the appropriate area on CHB and aluminium sink is fixed over it. By completely loosening and tightening the screws, applied pressure on thermal interface material is varied. An air blower (BL) is fixed over the heat sink with the help of adjusting guide (AG) to dispel the heat absorbed by the sink to the atmosphere. Difference between CHB temperature and room temperature is recorded during experimentation at decided power inputs. Rotational speed of the air blower was measured using anemometer and found to be 6.8 m/s. The recorded data (DL) is interfaced to PC for further simulations. Figure 6 Shows the indegenously fabricated instrumentation of Thermal Interface Material Set-up.

RESULTS AND DISCUSSION

Effective thermal contact resistance ($R_{th,\ eff}$) based on the fabricated set up is calculated as

$$(\mathrm{Rth, eff}) = (T2 - T1)℃/P\ (watts)$$

Where T_2 and T_1 represent the heater temperature and ambient temperature and p is the applied power.

Variation of Heater with Time and Pressure

Firstly, the temperature of CHB was measured on appropriate time intervals without thermal interface material

applied between the interfacing surfaces as depicted in figure 7 (A1-A2) to particularly determine the effective thermal contact resistance of CHB. Secondly, in the similar experimental conditions temperature variation of only base fluid was determined as given in figure 7 (B1-B2). Figure 7 (C1-C2) to 7 (G1-G2) gives the variation of the CHB temperature at appropriate time interval for different TIM at (RP) and (FP) which includes only base fluid and composites of base fluid and individual nanoparticles (SiO_2, Al_2O_3, CuO, GO and rGO) based TIM. Power inputs were changed as 25W, 50W and75W for study. Effective thermal contact resistance of all the samples were compared using graphs at full pressure and reduced pressure which is depicted from figure 8 to 13. ($R_{th,\ eff}$) is significantly less for nanoparticle and base fluid solution compared to base fluids alone. A rather significant observation is made that at full pressure ($R_{th,\ eff}$) for all materials is ver low as compared to the value at reduced pressure reinforcing the importance of bond line thickness in assessing thermal performance of TIM.

The graphs for without any interface material for both full pressure and reduced pressure depicts very less transmission of heat from heater to sink at various temperature levels and time depicting the need for interface material as the gap between heat and sink is prominent and increases the effective thermal contact resistance.The presence of base fluid does make a small difference in the reduction of heater temperature over the time compared to the reading of without any interface material. The reason can be

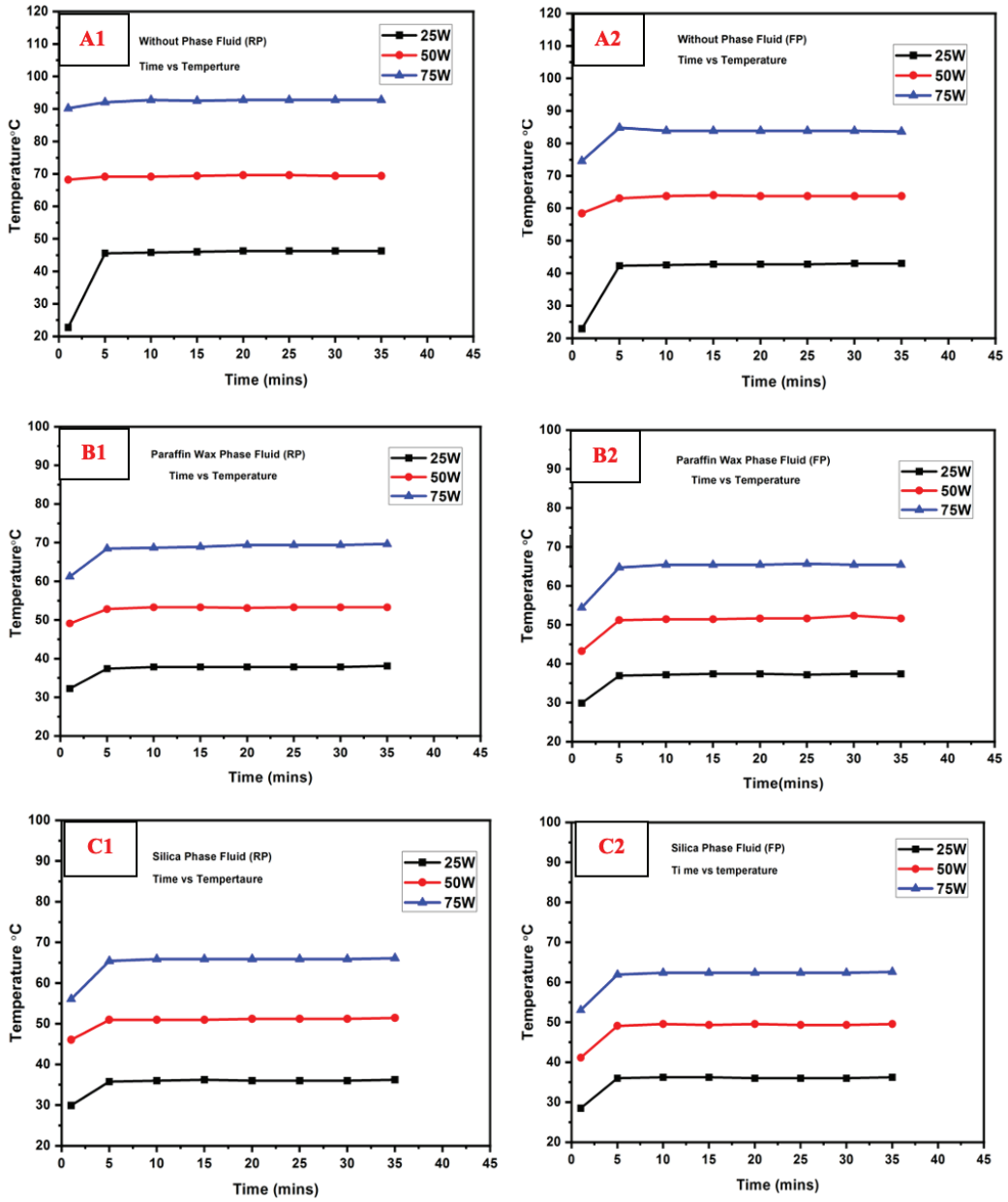

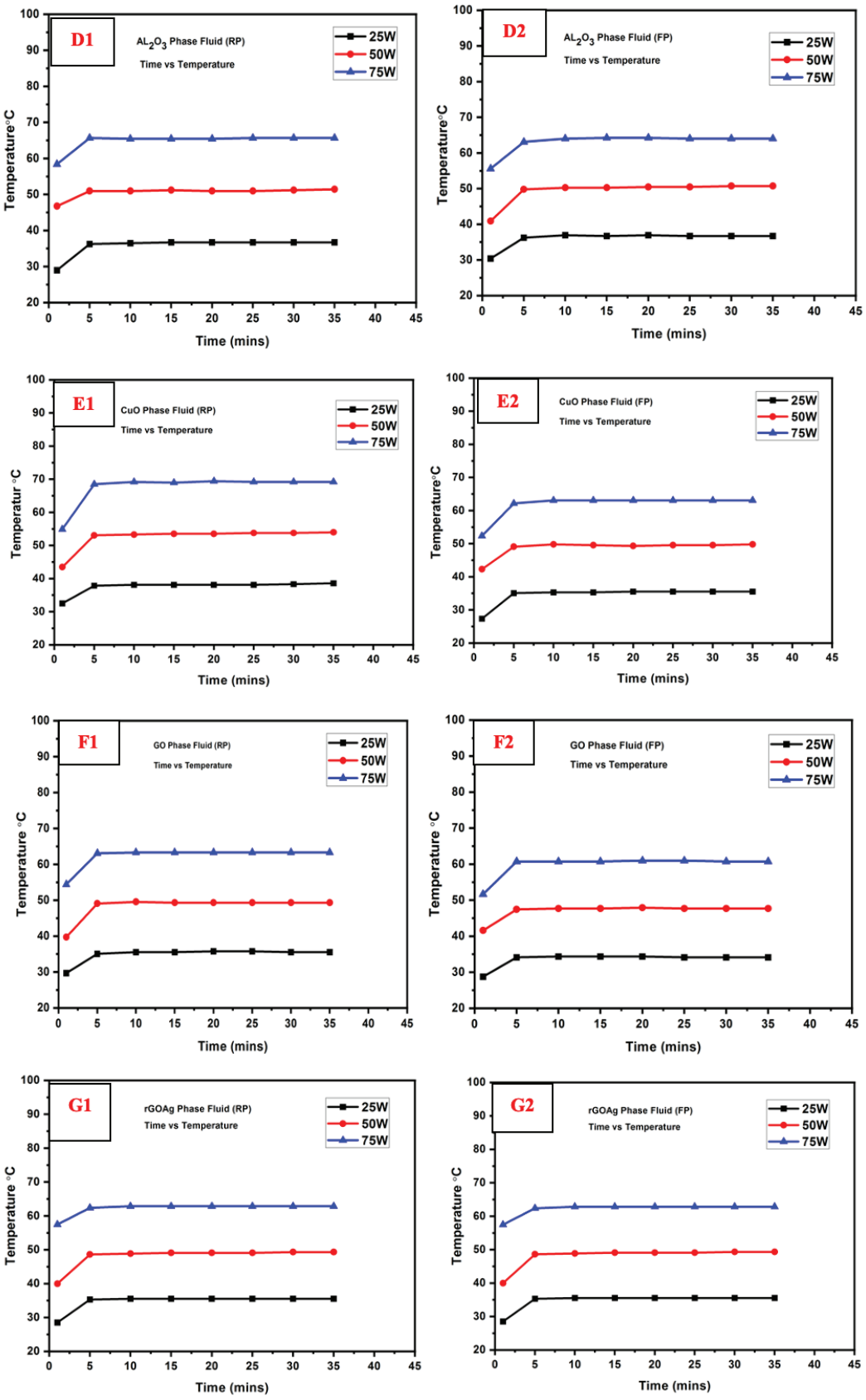

Figure 7. (A1-A2) , (B1-B2), (C1-C2), (D1-D2), (E1-E2), (F1-F2) and (G1-G2) represents Graph of time Vs heater temperature for without any interfcae material, paraffin wax, SiO_2, Al_2O_3, CuO, GO, rGO at difference power inputs of 25W, 50W and 75W and at full pressure (FP) and reduced (RP).

attributed to filling of microgaps and the contact between heater and sink, which aids in better flow of heat and hence reduction of effective thermal contact resistance to some extent. Here now the challenge is to improve the thermal conductivity of interface material for better results.

It is cleary observable from all the above graphs that heat dispelling capability is highest for all the nanoparticles based Tim at full pressure. The decreasing trend of (R_{th}, $_{eff}$) at full pressure can be atributed to decreasing bond line thickness and enhanced contact between TIM and aluminium sink which helps in good evacuation of heat.

Effective Thermal Contact Resistance of Nanoparticles Based TIM

Effective thermal contact resisntance for optimized 6 wt% of (SiO_2, Al_2O_3, CuO, GO and rGO) nanoparticles mixed in 5ml of paraffin wax was determined at the power inputs of 25W, 50W and 75W using the experimental set us given above.

From figure 8 to 13 represents the graphical depiction of effective thermal contact resistance of various TIM at different power inputs of (25 W, 50 W, 75 W), secondly at uniformily increasing time and at reduced pressure and full pressure. After the keen interpretation of the graphs it is deduced that time plays a mere role as not much difference is observed in the R_{th}, e_{ff}. After the initial escalation as the time increases the value almost stabilizes at a saturated point for all TIM and for all the varied power inputs.A major contribution to the steady raise of R_{th}, e_{ff} in all TIM was the increasing power input as it heats up the catridge according to the strength of applied power. It becomes an incumbent

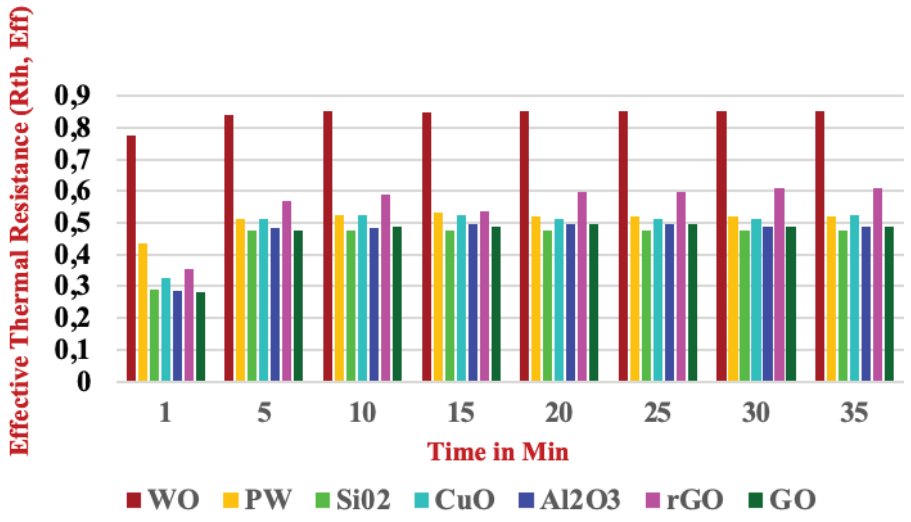

Figure 8. Comparison of different TIM at 25W input power at reduced pressure.

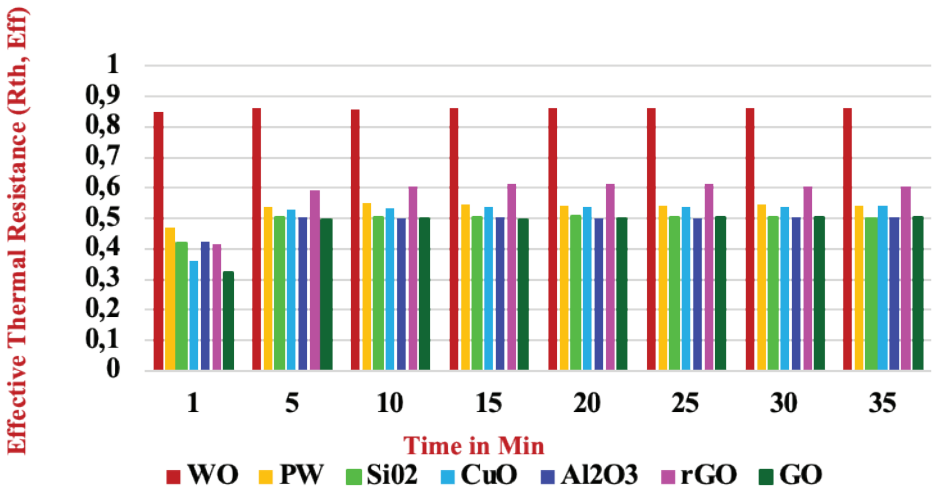

Figure 9. Comparison of different TIM at 50 W input power at reduced pressure.

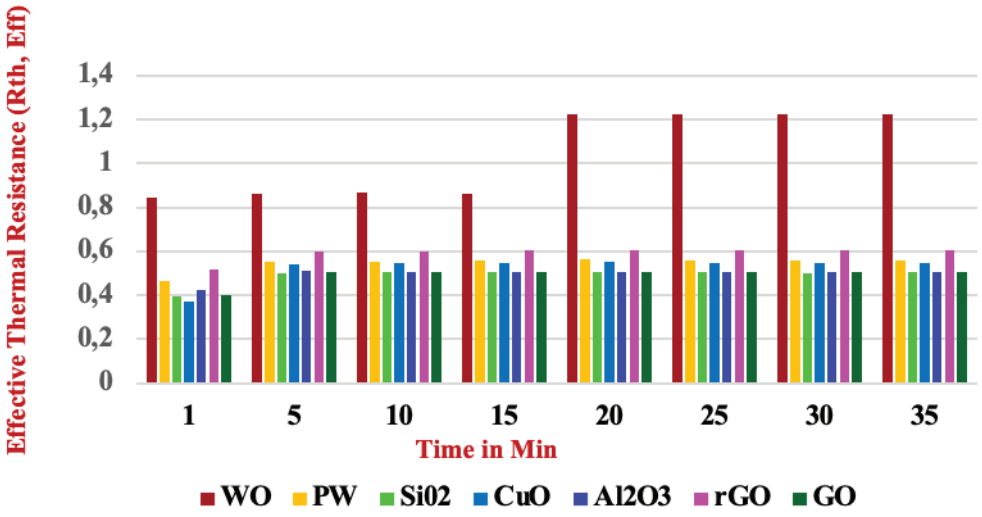

Figure 10. Comparison of different TIM at 75W input power at reduced pressure.

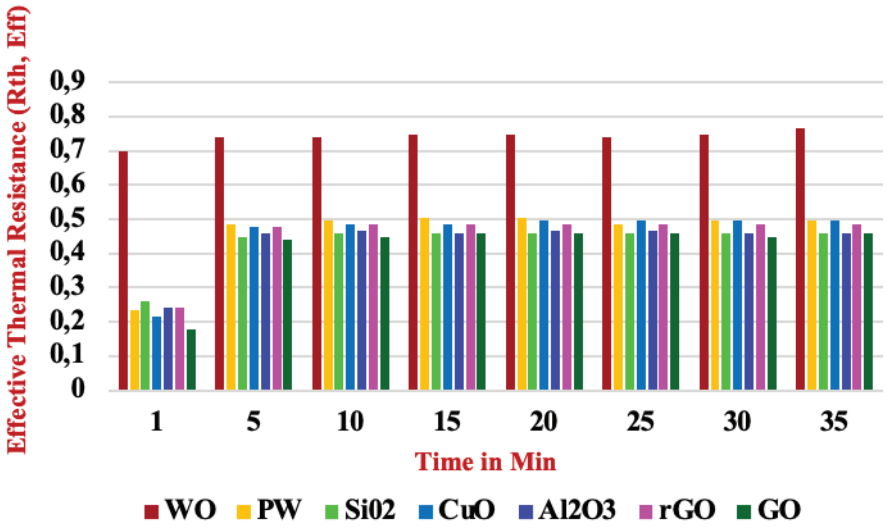

Figure 11. Comparison of different TIM at 25W input power at full pressure.

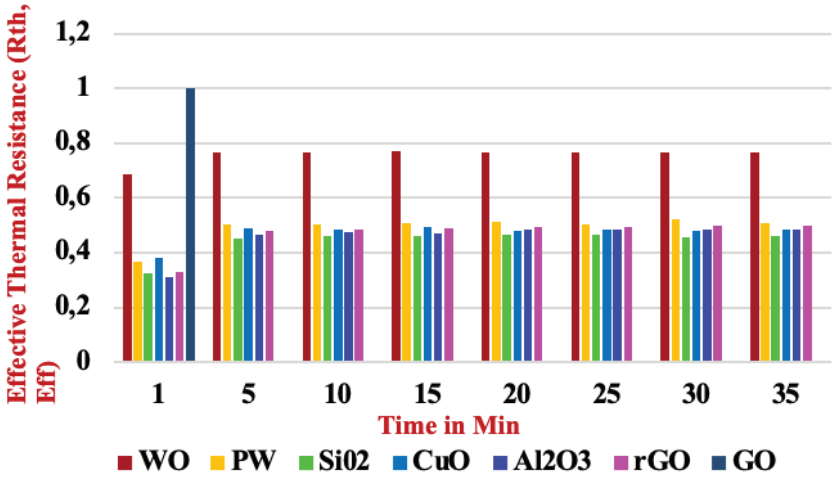

Figure 12. Comparison of different TIM at 50 W input power at full pressure.

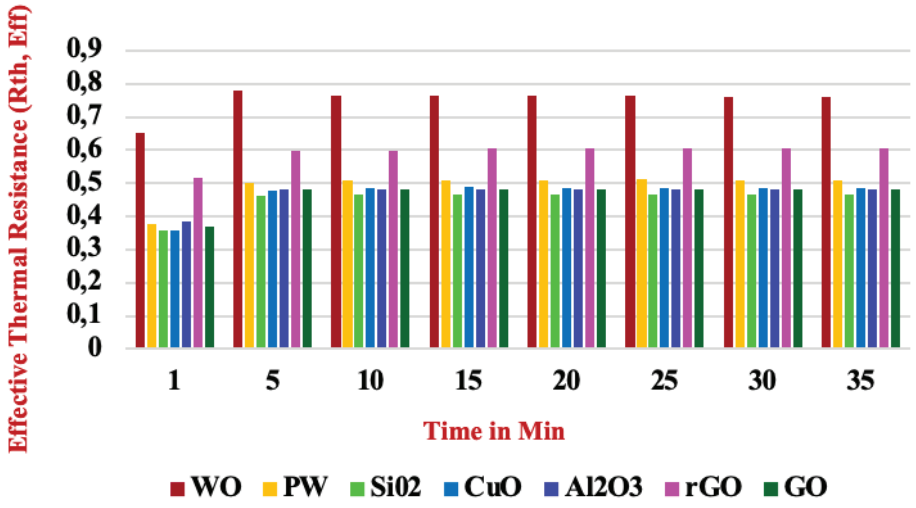

Figure 13. Comparison of different TIM at 75W input power at full pressure.

task to dissipate the heat from the electronic device as the power is raised. It is observed that R_{th}, e_{ff} values are significantly low after application of paraffin wax base fluid when compared to no base fluid condition. It is clearly evident that without base fluid the surface unevenness between the heater and sink is high and air fills the gap which has a very poor thermal conductivity of 0.025 W/m.K which resists the heat transfer. In this study, liquid paraffin wax was used which has a thermal conductivity of 0.3 W/m-K. It is hence validated that the base fluid fills that gap providing better heat transfer. Paraffin wax depicts 80% enhanced thermal conductivity compared to air. Further it is observed that addition of (SiO_2, Al_2O_3, CuO, GO and rGO) nanoparticles to the base fluid paraffin wax indeed decreases the effctive thermal resistance to a large extent. In order to obtained homogenous mixture of nanoparticles and base fluid, uniformly 6wt% of all (SiO_2, Al_2O_3, CuO, GO and rGO) nanoparticles was used for the present study. Noteworthy reduction in effective thermal resistance is observed as the incorporated nano parcticles helps in better heat conduction due to its higher surface area which enhances the thermal dissipation properly and further dipping in of effective thermal resistance ($R_{th, eff}$) is observed. Fistly we measured the without any base fluid and interface material readings at different power inputs of (25, 50 and 75W) at reduced pressure and full pressure. In the same manner readings were taken for the base fluid of 5ml paraffin wax and (SiO_2, Al_2O_3, CuO, GO and rGO) NPs sonicated and developed as a uniform paste-based TIM. Full pressure amounts to greater stress exerted at the sandwithced surface creating a closer interface between heat die and sink which helps in creating a conducive heat path. Hence, enhanced results are observed at full pressure.

In similar kind of research scientist have prepared nanofluids with base fluid DI water and filler particles Al_2O_3, SiO_2 and ZrO_2. Thermal conductivity of nanofluids enhanced with increment of volume concentration of filler particles and these three nanofluids exhibited enhanced thermal conductivity than base fluid DI water. Thermal conductivity of the DI water at room temperature of 30°C and found to be 0.6 W/mK. It was clearly visible that the thermal conductivity enhancement of 10.13% for Al_2O_3/H_2O, 6.5% for SiO_2/H_2O and 8.5% for ZrO_2/H_2O happened at 1% volume concentration [18]. Another highlighting observation is made that at reduced pressure ($R_{th, eff}$) escalates owing to poor gap filling and lack of fine bondline thickness. In depth evaluation of the presented graphical data gives an insight into the individual nanoparticle performance towards achiving superioir TIM. rGO unexpectedly fails in conducting the heat favorably as its effective thermal resistance were almost comparable to that of base fluid paraffin wax. The answer may lie in agglomeration or poor dispersive of rGO in paraffin wax which might have hindered the proper heat flow. SiO_2, CuO and Al_2O_3 give almost similar results. All the three filler materials are very good conductors of heat with proven high thermal conductivity factor. Maximum uncertainity measurement for results at 25 W was found around 3%.

Figure 14 and 15 depicts the average effective thermal contact resistance of different TIM at different power inputs and RP followed by FP. Its clearly evident that GO gives the best results as humange reduction of effective thermal resistance is observed for all the parameters. A Recent research showcases the fabrication of multilayer graphene–paraffin composite PCMs with different mass fractions. The thermal conductivities of composite PCMs enhanced with an increasing weight percentage of multilayer graphene. 10 wt % graphene in the PCM composite exhibited a 150% increase in thermal conductivity [19]. Our finding corroborates with the above stated research perfectly. Silica , CuO and Al_2O_3 give similar results.

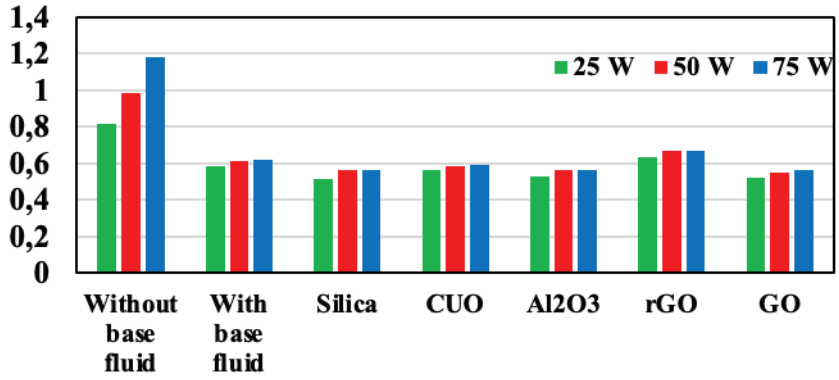

Figure 14. Comparison of average (Rth, Eeff) of different TIM at RP.

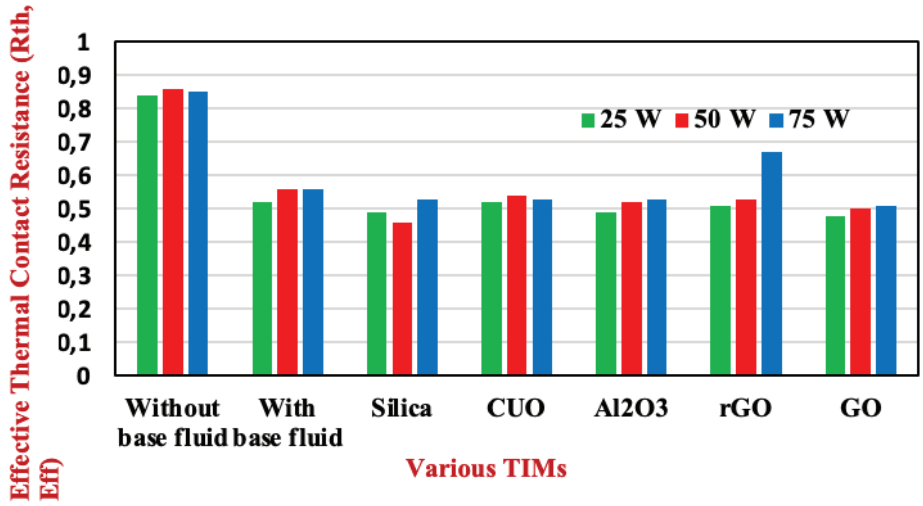

Figure 15. Comparison of average (Rth, Eeff) of different TIM at FP.

CONCLUSION

The present experimental study reports the relative study of effective thermal contact resistance ($R_{th,\,eff}$) measured for different thermal interface materials prepared as fine composite paste using paraffin wax as base fluid and SiO_2, Al_2O_3, CuO, GO and rGO as filler particles at different pressures, power inputs (25W, 50W and 75W) and time variations. In house built test rig using aluminium fin-based sink and copper heater was utilized to carry out heat dissipation experiments. It is clearly evident from the data that without any interface material the thermal contact resistance is observed to be highly escalated. The value at 75 W and FP is 0.85^{0}C/W, whereas when base fluid is added it drastically reduces to 0.6 ^{0}C/W. These results fortifies the need and importance of filling the uneven gap between heater and sink for proper dissipation of heat. As an overall observation, addition of nanoparticles (Al_2O_3, CuO, GO, rGO) in paraffin wax base fluid singnificantly improved the proper evacuation of heat and hence lower values of ($R_{th,\,eff}$) were observed in nanoparticles based TIM. Interestingly siliica based TIM gives the best performance of heat transference to ambience at 50 W power input ($R_{th,\,eff}$ = 0.46 ^{0}C/W) and slightly becomes inferior to GO at higher power input. Again instigating the researches to seriously ponder on the agglomerative behaviour of nanoparticles at higher temperature. This behaviour is observed at raised values of ($R_{th,\,eff}$) around 0.67 $^\circ$C/W for rGO based TIM, measured at 75 W and FP. GO based TIM shows the best results at higher power of 75 W, its $R_{th,\,eff}$ being 0.51 $^\circ$C/W reinforcing the behaviour of GO nanoparticle stability at high temperatures. Exceptions of results apart, at 75 W and FP conditions, all nanoparticle based TIMs have shown similar results for ($R_{th,\,eff}$) i.e 0.53 $^\circ$C/W for silica, CuO and Al_2O_3 based TIMs. Highlighting the importance of pressure on TIM, it was inferred from the findings that at full pressure ($R_{th,\,eff}$) lessens significantly for all samples.

NOMENCLATURE AND ABBREVIATION:

TIM	Thermal Interface Material
$R_{th,\,eff}$	Effective thermal contact resistance
RP	Reduced Pressure
FP	Full Pressure
WO	Represents the Without base fluid
PW	Represents the Paraffin wax base fluid
SiO_2	Represents the SiO_2 based TIM
CuO	Represents the CuO based TIM
Al_2O_3	Represents the Al_2O_3 based TIM
GO	Represents the GO based TIM
rGOAg	Represents the rGOAg based TIM
CHB	Copper Heater Block
HC	Heater Cartridge
AF	Aluminum Fins
TS	Thermal Sink
AC	Alternating Current
AS	Adjusting Screws
BL	Blower
AG	Adjusting guide for fan
SP	Spring for loading

HIGHLIGHTS

1. Nanoparticle based thermal interface materials prepared for electronic cooling application
2. TIM prepared with GO and aluminum nanoparticles gives the best results.
3. ($R_{th,\,eff}$) visibily decreases for all samples at full pressure which significantly tells the importance of bondline thickness.

ACKNOWLEDGMENTS

We are grateful to Karunya University for providing excellent facilities to carry out the entire research work. Also, I acknowledge the contribution of Mother Teresa Women's University, Kodaikanal in successfully accomplishing the research work.

AUTHORSHIP CONTRIBUTIONS

Authors equally contributed to this work.

DATA AVAILABILITY STATEMENT

The authors confirm that the data that supports the findings of this study are available within the article. Raw data that support the finding of this study are available from the corresponding author, upon reasonable request.

CONFLICT OF INTEREST

The author declared no potential conflicts of interest with respect to the research, authorship, and/or publication of this article.

ETHICS

There are no ethical issues with the publication of this manuscript.

STATEMENT ON THE USE OF ARTIFICIAL INTELLIGENCE

Artificial intelligence was not used in the preparation of the article.

REFERENCES

[1] Micheal HB, de sorgo M, John AM. Permalink Machine translation. 2005;US6054198

[2] Micheal HB, de sorgo M, John AM. Conformal thermal interface material for electronic components. 2000; US6054198.

[3] Prasher R. Thermal interface materials: historical perspective, status, and future directions. Proc IEEE. 2006; 94:1571-1586. [Crossref]

[4] Razeeb KM, Dalton E, Cross GLW, Robinson AJ. Present and future thermal interface materials for electronic devices. Int Mater Rev. 2018; 63:1-21. [Crossref]

[5] Mao D, Xie J, Sheng G, Ye H, Yuen MM, Fu XZ, Sun R, Wong CP. Aluminum coated spherical particles filled paraffin wax as a phase-change thermal interface materials. In: Proceedings of the 18th International Conference on Electronic Packaging Technology ;2017. pp 828-830. [Crossref]

[6] Bhanushali S, Ghosh PC, Simon GP, Cheng W. Copper nanowire-filled soft elastomer composites for applications as thermal interface materials. Adv Mater Interfaces 2017; 4:1700387. [Crossref]

[7] Lv L, Dai W, Yu J, Jiang N, Lin CT. A mini review: application of graphene paper in thermal interface materials. New Carbon Mater. 2021; 36:930-8. [Crossref]

[8] Shahil KMF, Balandin AA. Graphene-multilayer graphene nanocomposites as highly efficient thermal interface materials. Nano Lett. 2012; 2:861-7. [Crossref]

[9] Park W, Guo Y, Li X, Hu J, Liu L, Ruan X, et al. High-performance thermal interface material based on few-layer graphene composite. J Phys Chem C 2015;119:26753-26759. [Crossref]

[10] Sun Y, He Y, Tang B, Tao C, Ban J, Jiang L. Influence from the types of surface functional groups of RGO on the performances of thermal interface materials. RSC Adv 2017;7:55790. [Crossref]

[11] Schacht R, May D, Wunderle B, Wittler O, Gollhardt A, Michel B, et al. Characterization of thermal interface materials to support thermal simulation. 2007. arXiv:0709.1849v1 [Crossref]

[12] Tong T, Zhao Y, Delzeit L, Kashani A, Meyyappan M, Majumdar A. Dense vertically aligned multiwalled carbon nanotube arrays as thermal interface materials. IEEE Trans Compon Packag Manuf 2007;30:1. [Crossref]

[13] Narumanchi S, Mihalic M, Kelly K, Eesley G. Thermal interface materials for power electronics applications. 11th Intersociety Conference on Thermal and Thermomechanical Phenomena in Electronic Systems IEEE 2008;395-404. [Crossref]

[14] Yada S, Oyake T, Sakata M, Shiomi J. Filler-depletion layer adjacent to interface impacts performance of thermal interface material. AIP Adv 2016;6:015117. [Crossref]

[15] Guo Y, Yang X, Ruan K, Kong J, Dong M, Zhang J, et al. Reduced Graphene Oxide Heterostructured Silver Nanoparticles Significantly Enhanced Thermal Conductivities in Hot-Pressed Electrospun Polyimide Nanocomposites. ACS Appl Mater Interfaces 2019;11:25465-73. [Crossref]

[16] Chung DDL. Thermal Interface Materials. J Mater Eng Perform 2001;10:56-59. [Crossref]

[17] Maheshwari SU, Pillai BC, Govindan K, Raja M, Raja A, Pravin MBS, et al. Development of Low Resistance Thermal Interface Material (TIM) Using Nanomaterials. Int J of Eng Sci Inv 2018;2319-6734:39-46.

[18] Iqbal SM, Raj CS, Michael JJ, Irfan AM. A Comparative Investigation of Al_2O_3/H_2O, SiO_2/H_2O and ZrO_2/H_2O Nanofluid for Heat Transfer Applications. Digest J Nanomater Biostruct 2017;12:255-263.

[19] Balan AE, Sharea AA, Lavasani EJ, Tanasa E, Voinea S, Dobrica B et al. Paraffin-Multilayer Graphene Composite for Thermal Management in Electronics. Materials 2023;16:2-11. [Crossref]

Graphical abstract

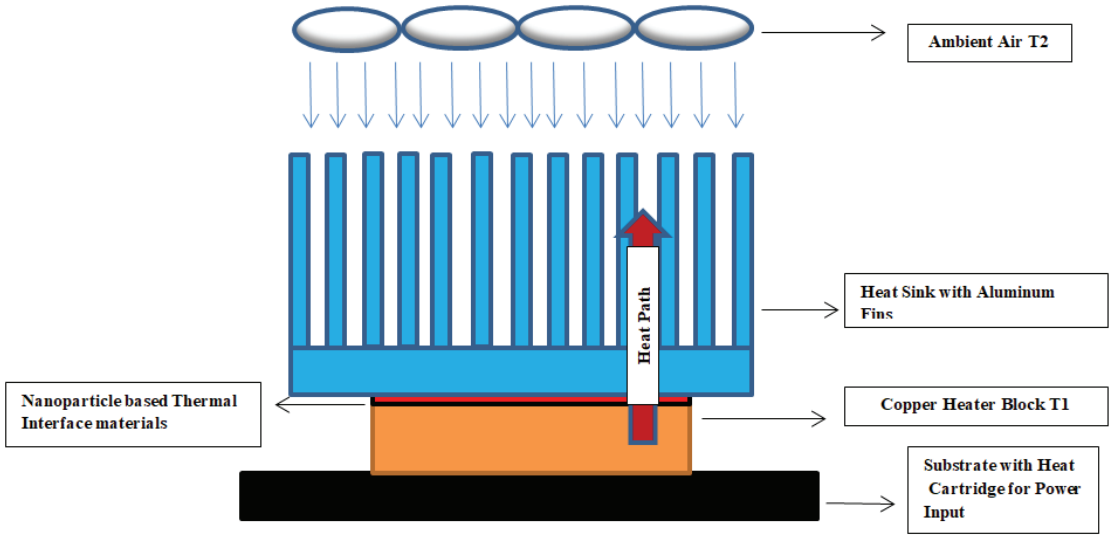

Principle of Effective Heat Transfer Using TIM